Cell PRESS
Immunity
Article

A Critical Role for STAT3 Transcription Factor Signaling in the Development and Maintenance of Human T Cell Memory

Andrea M. Siegel,[1] Jennifer Heimall,[2,8] Alexandra F. Freeman,[2] Amy P. Hsu,[2] Erica Brittain,[3] Jason M. Brenchley,[4] Daniel C. Douek,[5] Gary H. Fahle,[7] Jeffrey I. Cohen,[6] Steven M. Holland,[2] and Joshua D. Milner[1,*]
[1]Laboratory of Allergic Diseases
[2]Laboratory of Clinical Infectious Diseases
[3]Biostatistics Research Branch
[4]Laboratory of Molecular Microbiology
[5]Human Immunology Section, Vaccine Research Center
[6]Laboratory of Infectious Diseases
National Institute of Allergy and Infectious Diseases, National Institutes of Health, Bethesda, MD 20892, USA
[7]Microbiology Service, Division of Laboratory Medicine, Warren Grant Magnuson Clinical Center, National Institutes of Health, Bethesda, MD 20892, USA
[8]Present address: Division of Allergy/Immunology, The Children's Hospital of Philadelphia, Philadelphia, PA 19104, USA
*Correspondence: jdmilner@niaid.nih.gov
DOI 10.1016/j.immuni.2011.09.016

SUMMARY

STAT3 transcription factor signaling in specific T helper cell differentiation has been well described, although the broader roles for STAT3 in lymphocyte memory are less clear. Patients with autosomal-dominant hyper-IgE syndrome (AD-HIES) carry dominant-negative STAT3 mutations and are susceptible to a variety of bacterial and fungal infections. We found that AD-HIES patients have a cell-intrinsic defect in the number of central memory $CD4^+$ and $CD8^+$ T cells compared to healthy controls. Naive T cells from AD-HIES patients had lower expression of memory-related transcription factors *BCL6* and *SOCS3*, a primary proliferation defect, and they failed to acquire central memory-like surface phenotypes in vitro. AD-HIES patients showed a decreased ability to control varicella zoster virus (VZV) and Epstein-Barr virus (EBV) latency, and T cell memory to both of these viruses was compromised. These data point to a specific role for STAT3 in human central memory T cell formation and in control of certain chronic viruses.

INTRODUCTION

T cell memory is critical to the maintenance of immunity against many common pathogens. An understanding of how T cell memory is generated and maintained is necessary to design rational therapies and vaccines to protect against infections. T cell receptor signal strength, costimulation, and the presence of cytokines all contribute to differentiation of naive T cells into effector cells and memory cells (Cui and Kaech, 2010). In humans, it is thought that central memory T cells can home to the lymphoid organs and provide long-term T cell immunity through self-renewal, whereas effector memory T cells migrate to the periphery where they rapidly respond to secondary antigen exposure (Sallusto et al., 2010). The precise ontogeny of these populations along with the specific types of infections and pathogens against which they protect is not entirely understood.

Signal transducer and activator of transcription-3 (STAT3) is a latent cytoplasmic transcription factor with a wide variety of functions in mammalian cells (Levy and Lee, 2002). Within the immune system, STAT3 functions are noted in T cells, B cells, neutrophils, and macrophages among others. Particular attention has been paid to the effects of STAT3 on T and B cell maturation, differentiation, and function. The differentiation of several $CD4^+$ helper T (Th) cell subsets including Th17 cells, follicular helper T cells, and possibly Th2 cells appears to be dependent upon STAT3 (Eddahri et al., 2009; Nurieva et al., 2008; Vogelzang et al., 2008; Yang et al., 2007). Mice lacking STAT3 within the $CD4^+$ T cell compartment demonstrate impaired antifungal and antibacterial responses, poor germinal center formation, and defects in antibody production (Conti et al., 2009; Eddahri et al., 2009; Nurieva et al., 2008).

Several STAT3-dependent cytokines and transcription factors have critical roles in shaping $CD8^+$ T cell memory responses in mouse models. IL-21 signaling, which depends on STAT3, promotes memory formation, sustained functionality, and, ultimately, viral clearance during chronic lymphocytic choriomeningitis virus (LCMV) infection (Elsaesser et al., 2009; Fröhlich et al., 2009; Yi et al., 2009). IL-10-deficient mice infected with *Listeria monocytogenes* generate reduced numbers of memory T cells that fail to protect upon secondary challenge (Foulds et al., 2006). Other mouse models have revealed a critical role for STAT3-regulated transcription factors Blimp-1 (encoded by *PRDM1*) and Bcl6 (*BCL6*), both of which tend to counterregulate the other, in the generation of effector and central memory CD8 T cells, respectively (Ichii et al., 2002, 2004; Kallies et al., 2009; Rutishauser et al., 2009; Shin et al., 2009). Recent work has demonstrated an important role for SOCS3 in the control of chronic LCMV infections downstream of IL-6 signaling (Pellegrini et al., 2011). The direct mechanistic role the STAT3 pathway plays

in human effector and central memory T cell generation and its role in $CD4^+$ T cell memory in particular is not well understood.

Autosomal-dominant hyper-IgE syndrome (AD-HIES) is caused by dominant-negative *STAT3* mutations and is characterized by recurrent mucocutaneous candidiasis, staphylococcal skin and lung infections, dermatitis, elevated IgE, and a variety of skeletal and connective tissue abnormalities (Holland et al., 2007; Minegishi et al., 2007). Lymphocyte abnormalities previously observed in AD-HIES patients include defective Th17 cell differentiation (de Beaucoudrey et al., 2008; Ma et al., 2008; Milner et al., 2008; Renner et al., 2008), decreased $CD45RA^-$ T cells in children compared to normal adults (Buckley et al., 1991; Young et al., 2007), decreased memory B cells (Speckmann et al., 2008), and an increased risk for Epstein-Barr virus (EBV)-positive and EBV-negative lymphoma formation (Kumánovics et al., 2010).

We used the opportunity presented by STAT3 mutant AD-HIES patients to examine the role of STAT3 in the generation and maintenance of lymphocyte memory. We found that these patients had increased numbers of naive T cells and fewer central memory $CD4^+$ and $CD8^+$ T cells despite enhanced cell turnover in the absence of increased cell death. This observation appeared to be due to a defect in proliferation and differentiation from naive precursors and diminished expression within the naive compartment of transcription factors important for memory differentiation. As a potential consequence of the memory defects, HIES patients were found to have a previously unrecognized predisposition to develop varicella zoster virus (VZV) reactivation and EBV viremia.

RESULTS

Patients with AD-HIES Have Fewer Central Memory T Cells

We recruited a cohort of 19 AD-HIES patients and 10 age-matched healthy controls (ages 30–56) with mutations in the SH2, DNA binding, and transactivation domain of STAT3. We observed a decrease in the frequency of $CD4^+$ and $CD8^+$ central memory ($CD3^+CD27^+CD45RO^+$) T cells in AD-HIES patients compared to controls (Figure 1A). The total numbers of $CD4^+$ and $CD8^+$ central memory ($CD3^+CD27^+CD45RO^+$) T cells were significantly decreased in the AD-HIES patients (mean reduction of 45% in the $CD4^+$ subset and 60% in the $CD8^+$ subset) (Figure 1B). A corresponding increase was observed in the number of naive ($CD27^+CD45RO^-$) T cells in AD-HIES patients (Figure 1C). When compared to wild-type naive T cells, the $CD27^+CD45RO^-$ T cells from AD-HIES patients had similar expression of CD31, a marker of recent thymic emigrants (Figure S1A available online). Sorted $CD31^+CD27^+CD45RO^-$ CD4 and CD8 T cells from AD-HIES and control patients had similar numbers of T cell receptor excision circles (TRECs) and were consistent with previous reports in normal subjects (Figure S1B; Kimmig et al., 2002). Additionally, CD28 expression and decreased expression of CD11a were similar in AD-HIES and control $CD27^+CD45RO^-CD4^+$ T cells (Figure S1C). Thus, AD-HIES $CD27^+CD45RO^-CD4^+$ T cells appear to be phenotypically and functionally naive.

Effector memory ($CD3^+CD27^-CD45RO^{+/-}$) T cell numbers were similar in both AD-HIES patients and controls (Figure S1D). CD127, an important central memory surface marker (Kaech et al., 2003), was lower in AD-HIES central memory T cells (Figures 1D, 1E, and S1E). Similar to recent clinical findings, we have not noted any correlation between the genotype of the AD-HIES patients and observed the central memory phenotype (Heimall et al., 2011). Patients with HIES therefore have a focal diminution in T cells with a central memory phenotype coupled with an apparent accumulation of naive T cells.

AD-HIES T Cells Have an Intrinsic Defect in Memory Differentiation

We next examined whether the observed defect in central memory T cell differentiation was intrinsic to the $CD4^+$ and/or $CD8^+$ T cells as opposed to a failure of help from other cellular sources or soluble mediators. A patient was identified with normal frequencies of central memory $CD4^+$ and $CD8^+$ T cells, yet they had two children with germline *STAT3* mutations and abnormal central memory T cell counts (Figure 2A). The patient was found to be mosaic for an AD-HIES *STAT3* mutation (Figure 2B and data not shown). Quantitative PCR measurement of the mutant *STAT3* allele (*G1145ASTAT3*) from the AD-HIES mosaic patient found detectable mutant allele in the patient's naive $CD4^+$ and $CD8^+$ T cells but not in their central or effector memory T cells (Figures 2B and 2C). As a control, the frequency of an unlinked single-nucleotide polymorphism (SNP) was determined to be 50% of alleles in naive as well as memory T cell populations (Figure 2B). Of note, memory B cells from the mosaic patient had the same frequency of mutant *STAT3* allele as naive B cells, arguing against a B cell-intrinsic defect, and suggesting that a different mechanism underlies the B cell memory deficit observed in AD-HIES (Figures 2D and S2B; Avery et al., 2010). The T cell-intrinsic memory defect appears to be due in part to enhanced reliance upon IL-2 because in vitro expansion of sorted naive $CD4^+$ T cells from the *STAT3* mosaic patient in the presence of IL-2Rα (Daclizumab) antibody resulted in a marked reduction of mutant *STAT3* allele frequency after 10 days in culture (Figure 2E). Thus the T cell memory defect in AD-HIES appears to be cell intrinsic, potentially resulting from increased reliance upon IL-2, whereas the B cell memory deficiency is not cell intrinsic.

Decrease in Central Memory T Cells in AD-HIES Is Not due to Differences in Apoptosis or Turnover

We investigated further the mechanisms for the reduction in central memory T cells in AD-HIES. The frequency of naive and memory apoptotic T cells from 48 hr in vitro incubation was not significantly different between AD-HIES and control cells, suggesting that death was not increased (Figure 3A). Cell turnover in vivo as measured by Ki67 expression in the T cell subsets was not diminished, either (Figures 3B and 3C). Interestingly, turnover increased in the central memory and $CD4^+$ T cell effector memory compartment of AD-HIES patients (Figures 3B and 3C). This increased cell turnover may be a homeostatic response to the relative reduction in central memory T cells, an interpretation supported in part by a detectable increase in serum IL-15 concentrations in AD-HIES patients (Figure 3D). No significant difference in IL-2 or IL-7 concentrations was observed in AD-HIES patients (Figure 3D). Therefore, the central memory defect in AD-HIES patients would not appear to be due

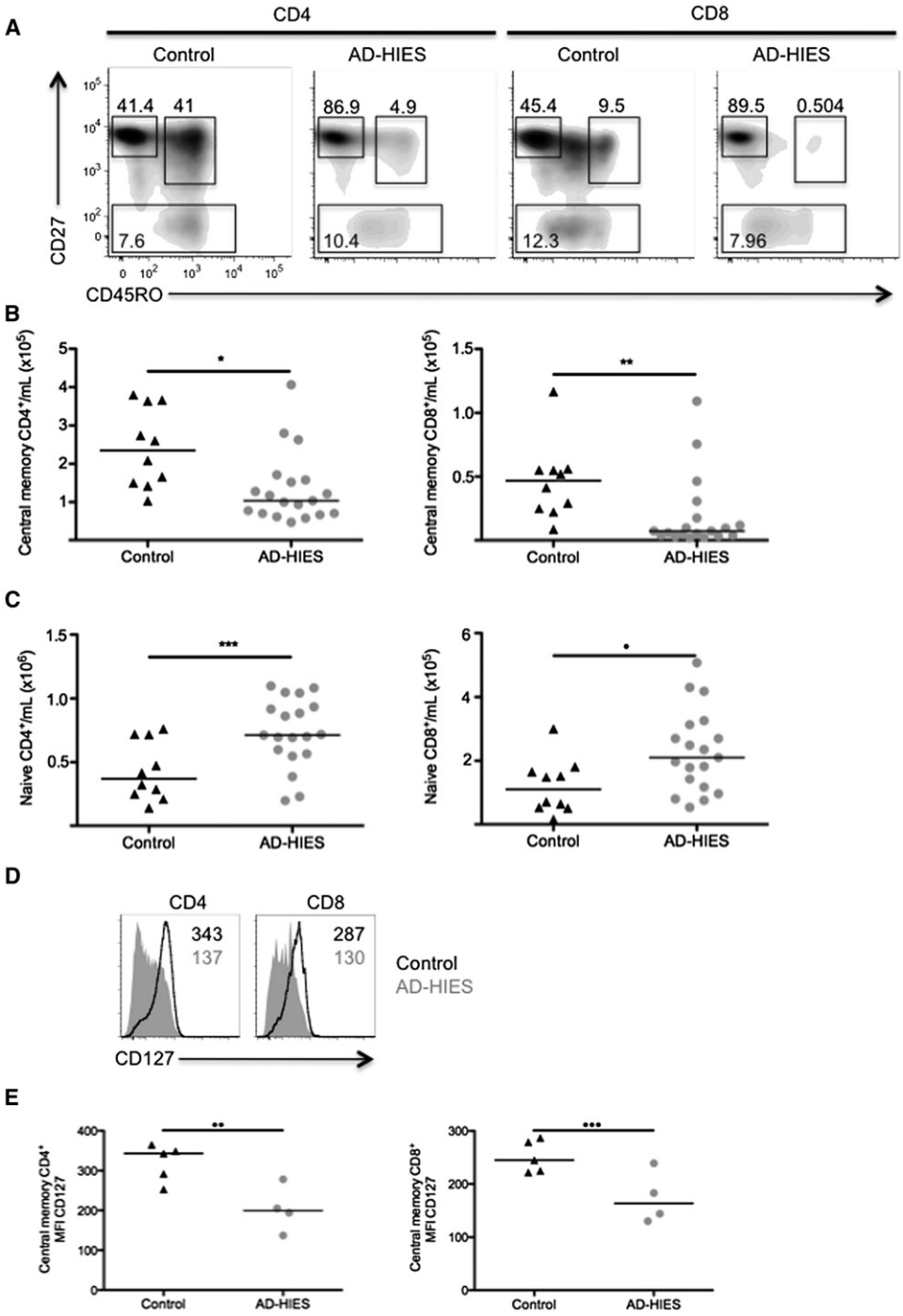

Figure 1. Patients with AD-HIES Have Fewer Central Memory T Cells

(A) The frequencies of naive ($CD27^+CD45RO^-$), central ($CD27^+CD45RO^+$), and effector ($CD27^-CD45RO^{+/-}$) memory T cells were measured in AD-HIES patients and healthy age-matched controls by flow cytometry. Representative graphs and gating from age-matched subjects. Cells are gated singlet, aqua viability$^-CD3^+$.

(B) Absolute lymphocyte counts were used to calculate the number of central memory lymphocytes in each population. *p = 0.0083, **p = 0.0036.

(C) A concomitant increase in the number of naive ($CD27^+CD45RO^-$) T cells was observed in AD-HIES patients. Data are compiled from seven independent experiments. ***p = 0.0261, *p = 0.0160.

(D and E) CD127 expression on central memory ($CD27^+CD45RO^+$) T cells was measured by flow cytometry.

(D) Representative histograms of CD127 expression on $CD27^+CD45RO^+$ central memory T cells.

(E) Mean fluorescence intensity of CD127 on the surface of central memory AD-HIES T cells was lower than that of control cells. **p = 0.0317, ***p = 0.0635. Data are representative of two similar experiments. All horizontal bars represent median values, and significance was calculated with a two-tailed Mann-Whitney t test with a 95% confidence interval.

to increased cell death or failure of central memory T cells to turn over sufficiently in vivo, but an increased reliance upon IL-2 for competitive fitness as well as a variable initial effector response may contribute to the phenotype.

Impaired In Vitro Induction of Central Memory T Cell Phenotypes

Given the observed increase in naive T cells in AD-HIES patients and the decrease in CD127 expression within the central memory cells, we speculated that there might be a primary defect in the proliferation and differentiation of naive T cells into cells with central memory phenotypes. Cultures of sorted naive $CD4^+$ and $CD8^+$ T cells from most AD-HIES patients stimulated with anti-CD3 and anti-CD28 in the presence of IL-2 demonstrated impaired proliferation compared to healthy controls as measured by CFSE dilution and proportion of live blasting cells at the end of the culture (Figures 4A and S3A–S3C) Sorted naive T cells from two different samples obtained from a single AD-HIES patient cultured under the same conditions had similar blasting phenotypes when compared to their respective control, implying that the ability to blast may not be highly variable within each patient (data not shown). This defect would not appear to be due to impaired activation and upregulation of CD25 (Figure S3D) despite evidence in mice that T cells deficient in STAT3 fail to efficiently upregulate CD25 upon activation (Akaishi et al., 1998). Additionally, we observed no link between the domain of STAT3 mutated in the patient and their ability to blast in vitro.

IL-7 and IL-15 have been demonstrated to play key roles in memory T cell homeostasis and differentiation (Kaech et al., 2003; Ku et al., 2000; Peschon et al., 1994). Short-term in vitro stimulation and expansion of naive T cells in the presence of IL-2, IL-7, or IL-15 can lead to the differentiation into effector or central memory-like surface phenotypes in several mouse models, which correlate to their appropriate memory functions upon adoptive transfer (Carrio et al., 2004; Manjunath et al., 2001). Naive T cells from AD-HIES patients were similarly stimulated for 4 to 6 days in the presence of IL-2, IL-7 ($CD4^+$), or IL-15 ($CD8^+$). In at least four individual experiments with four different patients and controls, we found that those AD-HIES T cells that did divide had a reduction, in some cases marked, in the frequency of $CD45RO^+CD62L^{hi}$ cells (Figures 4C, 4D, and S4A) in the presence of IL-7 (CD4) or IL-15 (CD8). In most cultures, upregulation of CD45RO was decreased in AD-HIES patients as a function of division number compared to controls (Figure S4B). Of note, IL-2 treatment alone did not appear to drive an effector memory phenotype as seen in the mouse models, perhaps reflecting differences between the species (Figures S4C and S4D). Regardless, with this human in vitro model, division of activated naive T cells was markedly impaired, as was the capacity for dividing T cells with *STAT3* mutations to differentiate into a central memory-like phenotype.

Naive STAT3 Mutant T Cells Have Impaired Expression of Transcription Factors Related to Central Memory T Cell Differentiation

The impaired in vitro central memory differentiation was associated with decreased expression of two STAT3-responsive transcription factors important in the development of T cell memory, *BCL6* and *SOCS3* (Ichii et al., 2002, 2004; Pellegrini et al., 2011), within the naive T cell compartment of many AD-HIES patients (Figure 5A). The decreased presence of BCL6 and SOCS3 transcripts in AD-HIES naive T cells, coupled with the proliferation defect, may contribute to their decreased ability to become $CD45RO^+CD62L^{hi}$ in vitro as well as the increased naive T cell pool and the lower numbers of central memory cells found in vivo.

Central memory CD8 T cells had a more effector memory-like transcriptional profile in AD-HIES patients. In control subjects, *BCL6* was elevated in the central memory CD8 T cells and *PRDM1* was elevated in effector memory populations in a pattern similar to that seen in mouse models of memory T cell differentiation (Figures 5B and S5; Rutishauser et al., 2009). However, sorted ex vivo AD-HIES central memory T cells expressed less *BCL6* than controls, and effector memory cells expressed more *PRDM1* than controls (Figures 5B, 5C, and S5). The altered expression of these key transcription factors as well as the lower surface expression of CD127 also suggests that the fewer AD-HIES T cells that succeed in differentiating in vivo into central memory T cells do not possess a typical central memory T cell phenotype, which could therefore lead to defects in function independent of number. The failure to acquire central memory phenotypes may therefore be linked to impaired expression of STAT3-dependent transcription factors that are important for memory differentiation.

AD-HIES Patients Have an Increased Risk for VZV Reactivation and EBV Viremia

AD-HIES patients are highly susceptible to bacterial and fungal infections but appear to control primary viral infections normally (Freeman and Holland, 2010). In an attempt to find clinical correlates to the observed central memory T cell defects, we surveyed AD-HIES patients for evidence of impaired control of chronic viral infections. We found that nearly one third of AD-HIES patients had a history of reactivation of VZV (herpes zoster, shingles) at relatively young ages (Figure 6A and Table 1). Starting the second decade of life and onward, the incidence rates of reactivation were 20.6, 11.1, 17.6, and 70.2 cases, respectively, per 1000 person years (Table 1). These rates were 6- to 20-fold higher than the rate of herpes zoster in the general population (1 to 3 per 1000 person years) over the same decades of life (Donahue et al., 1995; Hope-Simpson, 1975; Yawn et al., 2007). The recurrence rate of herpes zoster in AD-HIES patients was 27.4 per 1000 person years after initial reactivation (5 of 19 patients, 26.3%), which is a substantial increase over the general population's estimated rate of 7.4 per 1000 person years (Donahue et al., 1995).

Although VZV-specific antibody titers in AD-HIES appear normal (Avery et al., 2010), we measured $CD4^+$ T cell responses to VZV given that these cellular responses appear to be the most tightly correlated to risk for reactivation (Burke et al., 1982). We found that the increased incidence of herpes zoster in AD-HIES patients was associated with a reduction in the number of memory $CD4^+$ T cells, which produced either IL-2, IFN-γ, or TNF-α in response to VZV-infected cell lysate compared to controls, regardless of patient history of VZV reactivation (Figures 6B and S6). The responding cell population was too small to differentiate central from effector memory phenotypes.

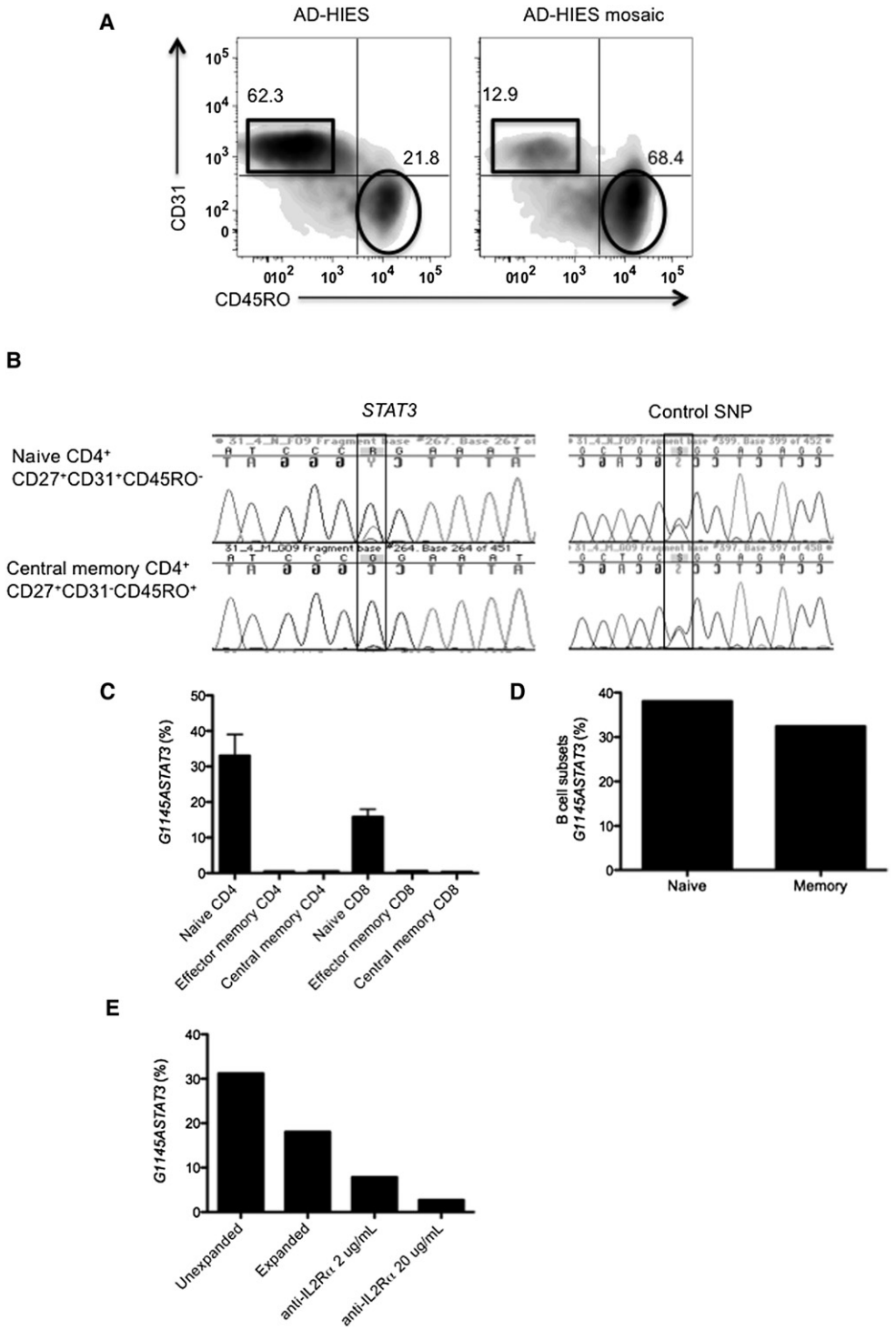

Figure 2. AD-HIES T Cells Have an Intrinsic Defect in Memory Differentiation

(A) The frequency of central memory $CD4^+$ T cells in a patient mosaic for an AD-HIES *STAT3* mutation (*G114ASTAT3*) and their AD-HIES child. Cells are gated $CD3^+CD4^+CD27^+$. Naive (rectangle, $CD27^+CD31^+CD45RO^-$) and central memory (circle, $CD27^+CD31^-CD45RO^+$) mosaic AD-HIES T cells were purified by flow cytometry and the frequency of *G1145ASTAT3* alleles determined by real-time PCR.

(B) Chromatographs of *STAT3* and a control SNP (intron 13, rs2293152) depict the relative presence of mutant and normal STAT3 alleles in the naive and memory $CD4^+$ population.

(C) Naive ($CD31^+CD27^+CD45RO^-$), central ($CD31^-CD27^+CD45RO^+$), and effector memory ($CD31^-CD27^+CD45RO^{+/-}$) $CD4^+$ and $CD8^+$ T cells were sorted from the mosaic AD-HIES patient and subjected to sequence-specific real-time PCR for the *G114ASTAT3* allele. Real-time PCR measurements of mutant *STAT3* alleles were measured in two independent experiments.

AD-HIES patients have an increased rate of lymphomas, a portion of which are EBV positive. We therefore measured EBV viremia and found that 54% of EBV antibody titer-positive AD-HIES patients had EBV$^+$ peripheral blood mononuclear cells (PBMCs) whereas only 14% of controls had detectable EBV DNA in the blood. AD-HIES EBV$^+$ PBMCs had markedly higher viral loads than EBV$^+$ controls (Figure 6C). Although the overall numbers of EBV-reactive memory CD4$^+$ and CD8$^+$ T cells were similar between AD-HIES patients and controls (Figure 6D), the EBV viremia observed in AD-HIES individuals was associated with lower frequencies of EBV-reactive central memory CD4$^+$ and CD8$^+$ T cells (Figures 6E and 6F). Cytomegalovirus (CMV) viremia, which can be better controlled when donor marrow is enriched for CMV-specific central memory T cells in transplant settings (Scheinberg et al., 2009), was not detected in the PMBCs of any AD-HIES patients or controls.

DISCUSSION

AD-HIES patients have decreased numbers of central memory T cells in part because of an intrinsic defect in their ability to proliferate and differentiate from naive precursors. Central memory CD8$^+$ T cells from AD-HIES patients had a more effector-like transcriptional profile, and both CD4$^+$ and CD8$^+$ central memory T cells had lower expression of CD127. The partial effacement of the central memory compartment in AD-HIES patients is associated with a failure to control VZV and EBV but appears to largely confer sufficient protection against other viruses, including CMV, which is seen only in more severe settings of T cell compromise such as bone marrow transplant, severe combined immunodeficiency, and advanced HIV (Kost and Straus, 1996; Steininger, 2007). Other congenital immune deficiencies characterized by mature B cell (Faulkner et al., 1999; Winkelstein et al., 2006), or Th17 cell defects (Ferwerda et al., 2009; Glocker et al., 2009; Puel et al., 2011) are not associated with abnormal VZV or EBV responses, arguing against a role for those defects that are normally observed in AD-HIES as a cause for the diminished capacity to control chronic viruses. Additionally, the relatively intact naive and effector memory pools may explain the failure to observe pathology from primary and recurrent viral infections in AD-HIES patients. This finding in AD-HIES appears unique in that no other known human immune deficiencies present from birth are characterized by increased rates of VZV reactivation in the absence of significant pathology when encountering primary VZV.

Our studies have revealed a role for STAT3 in CD4$^+$ and CD8$^+$ T cell memory separate from its role in T helper cell functional differentiation. *STAT3* mutations in AD-HIES patients demonstrate a critical role for STAT3 and STAT3-dependent transcription factors in the development of central memory in CD8$^+$ T cells and a previously unappreciated role for STAT3 in CD4$^+$ T cell central memory development. Of note, LCMV-infected *Gzmb*$^{Cre/+}$ *Stat3*$^{LoxP/LoxP}$ mice or mice with *Socs3* silenced in naive CD8$^+$ T cells have dramatically reduced frequencies of LCMV-specific central memory CD8$^+$ T cells memory (Cui et al., 2011, this issue). This work suggests that STAT3 signaling and *SOCS3* expression within naive T cells are key in steering CD8$^+$ differentiation away from an effector phenotype and toward long-term central memory. The proliferation defect observed in AD-HIES naive T cells could reflect a requirement for STAT3 pathway genes for normal naive T cell division (Durant et al., 2010) or the failure of STAT3 genes to counter antiproliferative effects of other STAT pathways such as the IL-27-STAT1 pathway (Liu and Rohowsky-Kochan, 2011). The variability in the capacity for different patients' naive cells to proliferate may stem from the fact that STAT3 mutations in AD-HIES are hypomorphic, as opposed to null mutations. This diminished but not absent function can lead to a wider clinical variability, as well as unstable cellular phenotypes such as the defects in neutrophil chemotaxis, which can at times even vary within an individual patient (Donabedian and Gallin, 1983).

These newly observed clinical findings in AD-HIES may have other implications as well. Given that atopic dermatitis is a cardinal feature of AD-HIES, STAT3 pathway defects may also help explain an observed increased frequency of VZV reactivation in patients with severe atopic dermatitis (Rystedt et al., 1986). Additionally, the lower frequency of EBV-specific central memory T cells in AD-HIES may explain the observed increase in the number of EBV$^+$ cells in the blood. Although activation of STAT3 is associated with lymphomagenesis (Bromberg et al., 1999; Migone et al., 1995; Yu et al., 1995), the paradoxical increase in risk for B cell lymphomas in these patients with a loss of STAT3 function now may be understood as resulting from poor immune control of latently infected cells. This loss of immune control may explain the EBV$^+$ lymphomas in AD-HIES and also may have effects on the overall control of tumorigenesis, which has been shown to be partially dependent on central memory T cells (Klebanoff et al., 2005). Patients with dysfunctional STAT3 signaling may need to be more closely monitored for control of VZV and EBV, and they may benefit clinically from early and perhaps frequently boosted VZV vaccination.

The specific defect in T cell central memory formation and associated loss of control of certain chronic viral infections we observed in AD-HIES illuminates our understanding of central memory T cell differentiation and the role of central memory T cells in immune responses. These insights may aid in the development of new monitoring and vaccination strategies for long-term control of chronic viral infections.

EXPERIMENTAL PROCEDURES

Subjects

AD-HIES patients and controls were enrolled under Institutional Review Board-approved protocol 00-I-0159. The diagnosis of AD-HIES was based on both phenotypic analysis (a clinical score of > 40) (Grimbacher et al., 1999) and genetic sequencing of the *STAT3* locus. Patients ranged in age from 2 to 58 years with a mean of 27 years. Males and females were equally

(D) Naive (CD19$^+$CD27^{lo}) and memory (CD19$^+$CD27^{hi}) B cells were sorted from the AD-HIES mosaic patient and the frequency of cells with the *G1145ASTAT3* allele was measured by real-time PCR.

(E) Naive (CD31$^+$CD27$^+$CD45RO$^+$) STAT3-mosaic CD4$^+$ T cells were stimulated with irradiated feeder cells, PHA, with or without anti-IL-2Rα (Daclizumab) for 10 days and mutant-*STAT3* transcripts measured.

Data are representative of two independent experiments. All error bars represent standard error of the mean.

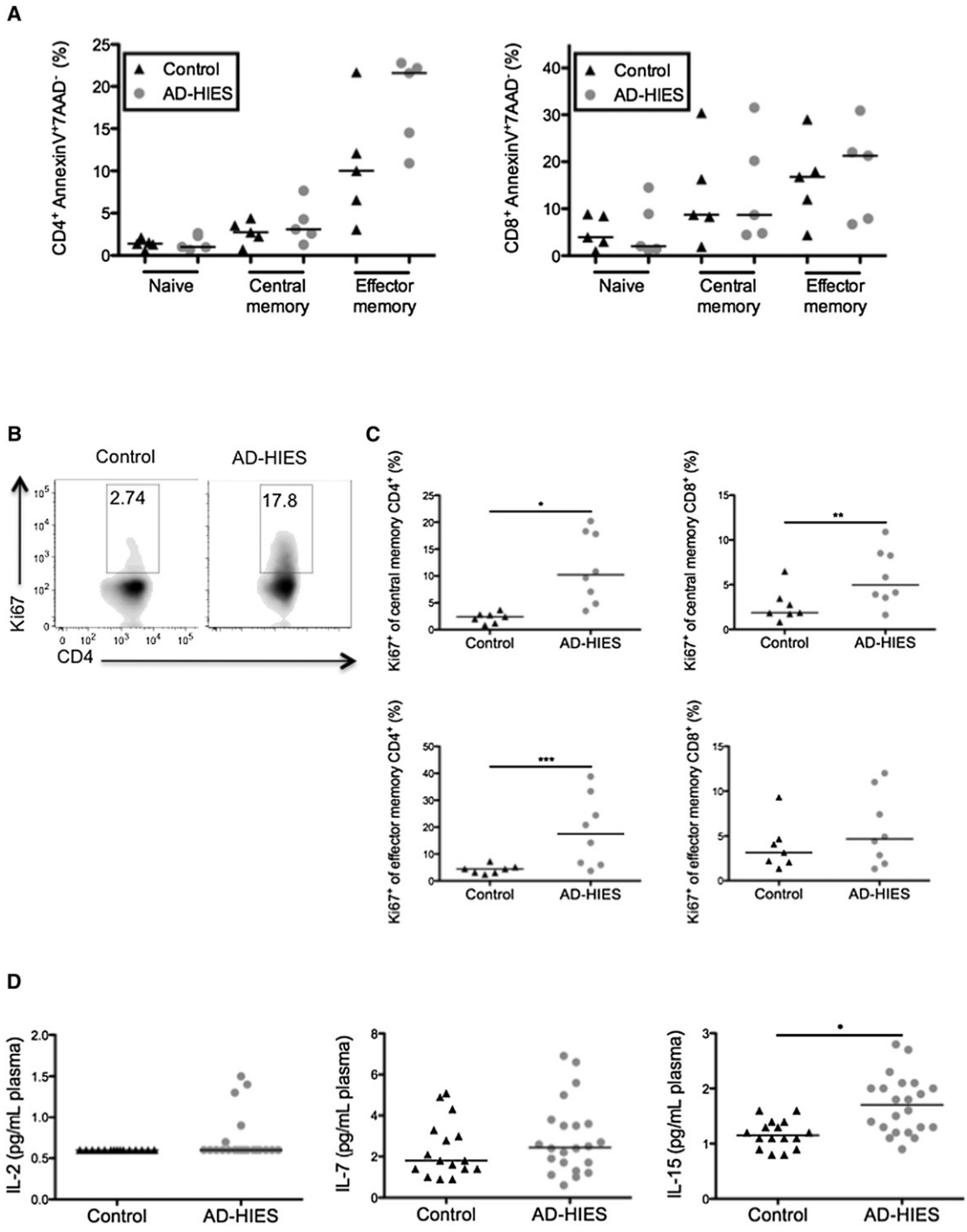

Figure 3. Decrease in Central Memory T Cells in AD-HIES Is Not due to Increased Ex Vivo Apoptosis or Decreased In Vivo Division

(A) PBMCs from five AD-HIES and five healthy controls were thawed and cultured in complete RPMI for 48 hr without stimulation or exogenous cytokine. The frequency of AnnexinV$^+$7AAD$^-$ cells was measured by flow cytometry in naive (CD27$^+$CD45RO$^-$), central (CD27$^+$CD45RO$^+$), and effector (CD27$^-$CD45RO$^{+/-}$) memory CD4$^+$ and CD8$^+$ subsets.

(B–D) Thawed PBMCs were stained for intracellular Ki67 and gated on CD27$^+$CD45RO$^+$ (central) and CD27$^-$CD45RO$^{+/-}$ (effector) T cells.

(B) Representative flow cytometry of Ki67 expression within CD4$^+$CD27$^+$CD45RO$^+$ central memory cells. Graphs depict singlet, aqua viability$^-$CD3$^+$CD4$^+$ CD27$^+$CD45RO$^+$ cells.

(C) Scatter plots depict Ki67 expression within central and effector T cell subsets of AD-HIES and control PBMCs from two independent experiments *p = 0.0006, **p = 0.0401, ***p = 0.0093.

(D) Serum levels of IL-2, IL-7, and IL-15 were measured by multiplex cytokine analysis. *p = 0.0014.

All horizontal bars represent median values, and significance was calculated with a two-tailed Mann-Whitney t test with a 95% confidence interval.

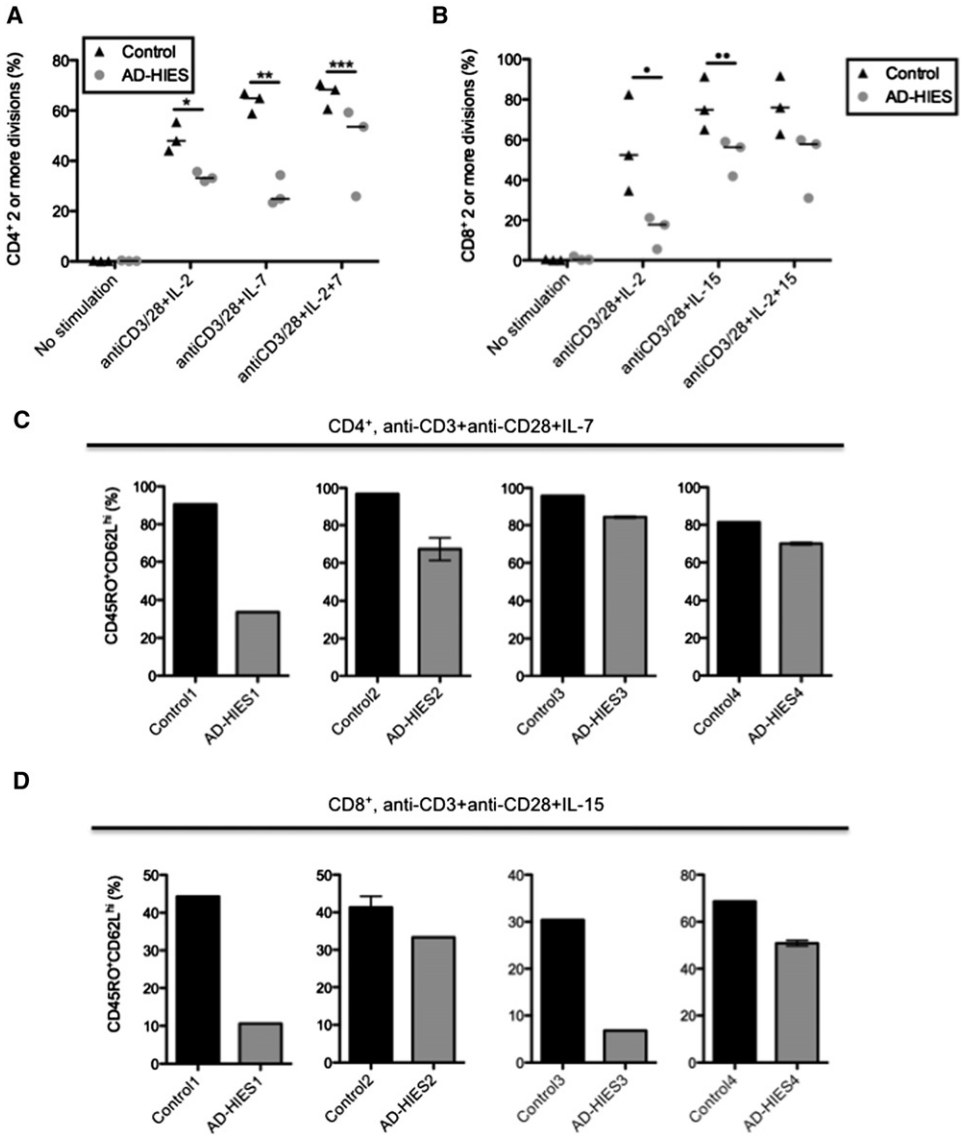

Figure 4. STAT3 Mutant Naive T Cells Have Impaired Proliferation and In Vitro Induction of Central Memory T Cell Phenotypes

(A) Sorted naive ($CD27^-CD45RO^-$) $CD4^+$ T cells were labeled with CFSE and cultured with anti-CD3 and anti-CD28 for 5 days in the presence of IL-2, IL-7, or IL-2 and IL-7. *p = 0.05, **p = 0.05, ***p = 0.05.

(B) Sorted naive ($CD27^-CD45RO^-$) $CD8^+$ T cells were labeled with CFSE and cultured with anti-CD3 and anti-CD28 for 5 days in the presence of IL-2, IL-15, or IL-2 and IL-15. *p = 0.05, **p = 0.05. All horizontal bars represent median values, and significance was calculated with a one-tailed Mann-Whitney t test with a 95% confidence interval.

(C and D) After 4 or 5 days, blasting or cells were analyzed for CD62L and CD45RO expression to determine differentiation status. Each bar graph represents an individual experiment with a unique control and AD-HIES pair. Error bars when present represent standard errors of the mean for cases when sufficient cells allowed for plating of multiple wells within a single experiment. Different controls and AD-HIES patients were assayed in each experiment.

represented. A total of 30 patients had mutations in the DNA binding domain, 27 had mutations in the SH2 domain, and 1 had a mutation in the transactivation domain of STAT3. Peripheral blood mononuclear cells were prepared from venous blood by Ficoll-gradient centrifugation and cryopreserved. Most patients were in a good health and admitted for annual well visits when samples were drawn.

Flow Cytometry

PBMCs were thawed, washed with PBS, and stained with aqua viability dye (Invitrogen, Carlsbad, CA) and the following surface and intracellular markers: CD3-Alexa700, CD8-PacificBlue, CD4-PECy5.5, -APC, CD27-FITC, -PECy5, CD4RO-TRPE, -PECy7, CD3-Alexa700, CD127-PE, CD62L-FITC, -V450, AnnexinV-FITC, -APC, 7AAD, Ki67-FITC, IL-2-APC, IFN-γ-FITC, TNF-α-PECy7 (all BD Biosciences, San Jose, CA). Events were collected on a LSRFortessa with Diva 6 software (BD Biosciences) and analyzed with FlowJo 9.1 and 9.3.1 software (Treestar, Ashland, OR). All plots gated on aqua negative (live) singlets excluding AnnexinV/7AAD staining. The CellTrace CFSE Cell Proliferation Kit (Invitrogen) was used according to the manufacturer's protocol. Intracellular cytokine staining was performed with Cytofix/cytoperm (BD Biosciences). The FoxP3 staining kit and protocol (eBioscience, San Diego, CA) was used to stain for Ki67-FITC (BD Biosciences). Populations were sorted with gating strategies specified in the legends on an Aria II cytometer (BD Biosciences).

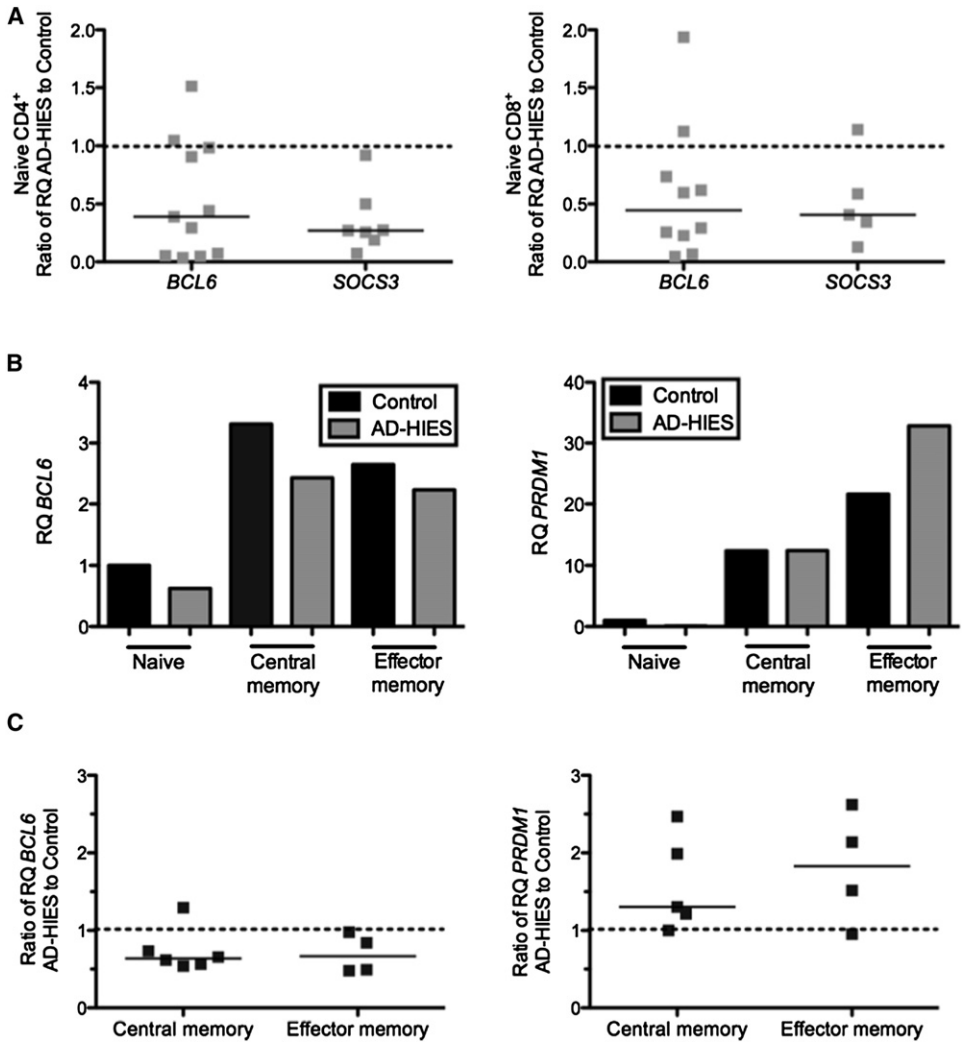

Figure 5. STAT3 Mutant Naive T Cells Have Decreased Central Memory-Related Transcription Factor Expression

(A) Naive ($CD27^+CD45RO^-$) $CD4^+$ and $CD8^+$ T cells were isolated from AD-HIES patients and controls by flow cytometry and transcript levels measured by real-time PCR. Each point represents the ratio of transcript observed in an AD-HIES patient compared to a corresponding healthy control subject. All data were collected from separate AD-HIES and control patients.

(B) Naive ($CD27^+CD45RO^-$), central memory ($CD27^+CD45RO^+$), and effector memory ($CD27^-CD45RO^{+/-}$) $CD8^+$ populations were purified by flow cytometry, and *BCL6* and *PRDM1* transcripts were measured by real-time PCR. Each set of $CD8^+$ populations was purified from a single individual. Data are representative of four independent experiments with four AD-HIES patients and four control subjects.

(C) Ratio of *BCL6* and *PRDM1* transcript levels between AD-HIES and control central and effector memory $CD8^+$ T cell populations. Each point represents the ratio of transcript observed in an AD-HIES patient compared to their corresponding normal control.

In Vitro Stimulation

Expansion of Mosaic T Cells

Naive T cells ($aqua^-CD3^+CD4^+CD27^+CD31^+CD45RO^-$ and $aqua^-CD3^+CD8^+CD27^+CD31^+CD45RO^-$) were purified by flow cytometry and cultured in RPMI (GIBCO, Carlsbad, CA) supplemented with 10% fetal calf serum (Gemini Bio-Products, West Sacramento, CA), 100 U/mL penicillin, 100 μg/mL streptomycin, and 29.2 μg/mL L-glutamine (all GIBCO) (complete RPMI) in the presence of irradiated PBMCs and purified phytohaemagglutinin (3 μg/mL, Remel Inc, Lenexa, KS) for 10 days. Anti-IL2Rα (i.e., Daclizumab, 2 or 20 μg/mL, Roche, Nutley, NJ) was added to cultures as indicated.

Memory T Cell Differentiation and Naive T Cell Stimulation

Naive ($aqua^-CD3^+CD4^+CD27^+CD45RO^-$ and $aqua^-CD3^+CD8^+CD27^+CD45RO^-$) T cells were purified by flow cytometry and cultured in complete RPMI for 4 to 6 days. Some cells were labeled with CFSE prior to culture. Cells were stimulated with anti-CD3 (OKT3) (1 μg/mL, eBioscience) and anti-CD28 (0.5 μg/mL, BD Biosciences) with the addition of recombinant human IL-2 (20 U/mL, Peprotech, Rocky Hill, NJ), IL-7 (25 ng/mL, a gift from C. Mackall), and IL-15 (100 ng/mL, Peprotech) as indicated.

Multiplex Cytokine Analysis

Plasma from patients and controls was tested for cytokine expression with the Meso Scale human assays for the indicated cytokines as per manufacturer's instructions (Meso Scale Discovery, Gaithersburg, MD).

PCR Analysis

TCR Rearrangement Excision Circle Analysis

Quantification of TCR rearrangement excision circle (TREC) in sorted $CD4^+$ and $CD8^+$ T cells was done by real-time quantitative PCR with the 5′-nuclease (TaqMan) assay and an ABI7700 system (Perkin-Elmer, Norwalk, CT) as previously reported (Douek et al., 2000). Cells were lysed in 100 mg/L proteinase K

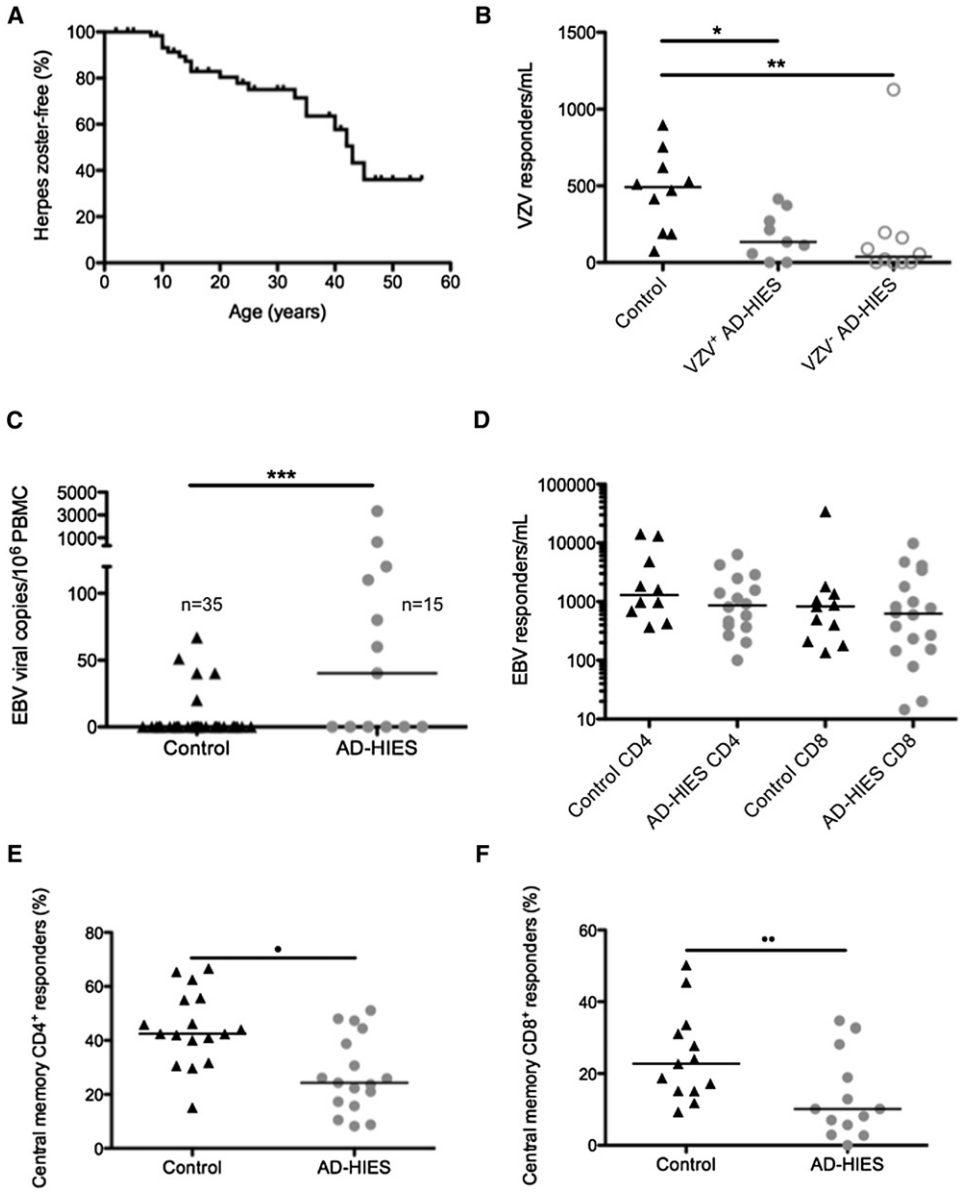

Figure 6. AD-HIES Patients Have an Increased Risk for VZV Reactivation and EBV Viremia along with Defects in Virus-Specific T Cell Memory

(A) Kaplan-Meier plot of incidence of herpes zoster (VZV reactivation) in AD-HIES cohort.

(B) Thawed PBMCs were stimulated with inactivated homogenate from VZV-infected cells and the sum of IFN-γ, TNF-α, and IL-2 production by total memory ($CD27^+CD45RO^+$ and $CD27^-CD45RO^{+/-}$) $CD4^+$ T cells was measured relative to unstimulated cells. Data are composite of seven independent experiments. *p = 0.0127, **p = 0.0089.

(C) The frequency of PBMCs harboring EBV genomes was determined by PCR assay. ***p = 0.0014.

(D) Thawed PBMCs were stimulated with inactivated lysate from EBV-infected cells and IFN-γ, TNF-α, and IL-2 levels in total memory ($CD27^+CD45RO^+$ and $CD27^-CD45RO^{+/-}$) $CD4^+$ and $CD8^+$ T cells were measured by flow cytometry.

(E and F) T cells that produced TNF-α and/or IFN-γ in response to EBV were analyzed for their surface expression of CD27 and CD45RO. Data compiled from seven independent experiments. *p = 0.004, **p = 0.0493. All horizontal bars represent median values, and significance calculated with a two-tailed Mann-Whitney t test with a 95% confidence interval.

(Boehringer, Indianapolis, IN) for 1 hr at 56°C, then 10 min at 95°C, at 107 cells/mL. Real-time quantitative PCR was done on 5 μl of cell lysate with the primers CACATCCCTTTCAACCATGCT and GCCAGCTGCAGGGTT TAGG and probe FAM-5′-ACACCTCTGGTTTTTGTAAAGGTGCCCACT-3′-TAMRA (MegaBases, Chicago, IL). PCR reactions contained 0.5 U Platinum taq polymerase (GIBCO, Grand Island, NY), 3.5 mmol/L $MgCl_2$, 0.2 mmol/L dNTPs, 500 nmol/L each primer, 150 nmol/L probe, and Blue-636 reference (MegaBases). Conditions were 95°C for 5 min, then 95°C for 30 s, 60°C for 1 min, for 40 cycles. A standard curve was plotted, and the numbers of TREC in samples were calculated by the ABI7700 software.

STAT3 Analysis

Cells sorted from the mosaic AD-HIES patient were washed in PBS and lysed in PureGene DNA Isolation Kit Cell Lysis Solution (Quiagen, Valencia, CA). Amplification of exons 12–14 of STAT3 was performed with 0.5 mM each

Table 1. Incidence of Herpes Zoster in AD-HIES

Age Group	Cases	Person Years	Rate per Year (95% CI)	Rate per 1000 Person Years (95% CI)
<10	1	608	0.0016 (0.000, 0.0092)	1.6 (0, 9.2)
10–19	8	399	0.0201 (0.0087, 0.0395)	20.1 (8.7, 39.5)
20–29	4	271	0.0111(0.0023, 0.0324)	11.1 (2.3, 32.4)
30–39	3	168	0.0179 (0.0037, 0.0522)	17.9 (3.7, 52.2)
40–49	3	57	0.0702 (0.0191, 0.1797)	70.2 (19.1, 179.7)
>50	0	8	0	0

primer, 12F amp- 5′-TAGTTTAAAGAAATGCCCAGGAGCACAGAGGTTTT-3′ and 14R amp- 5′-TTTGGCCTGAAGTGACTTTTTGGAATAACTACAGC-3′ with 10–100 ng of genomic DNA and Platinum Taq HiFidelity Supermix (Invitrogen). PCR products were analyzed on an agarose gel and purified with ExoSAP-IT (USB Corporation, Cleveland, OH). Sequencing was performed with Big Dye Terminators v3.1 (Applied Biosystems, Foster City, CA) and the following primers 13-14F 5′-CTGGGGACGTTGCAGCTCTCAGAGGGTAAGT-3′ and HpaII R 5′-CTCGGCCCCCATTCCCACATCTCT-3′. SNP genotyping primer probe sets for the known SNP in intron 13, rs2293152, and a custom pair designed to distinguish the 1145A mutation from the 1145G wild-type allele (Applied Biosystems) were used for quantitative PCR. Reactions were performed in triplicate with 20 μl volume with 10–100 ng DNA per reaction and 2 × reaction mix (Applied Biosystems).

Transcript Analysis

RNA was isolated with the RNeasy Mini Kit (Quiagen) as per manufacturer's instructions. cDNA was reverse transcribed with the High-Capacity cDNA Reverse Transcription Kit (Applied Biosystems). Triplicate real-time PCR reactions were performed with 20 μl volume with 2 × reaction mix and the following primers: 18S Hs99999901_s1, PRDM1 Hs00153357_m1, BCL6 Hs00277037_m1, and SOCS3 Hs01000485_g1 (Applied Biosystems). Transcripts were measured relative to 18S levels to normalize for cDNA input.

STAT3 and transcript PCR reactions underwent 40 cycles and were analyzed on an ABI 7500 Real Time Thermal Cycler (Applied Biosystems).

Viral Memory Response

PBMCs were thawed and rested in complete RPMI for 2 hr. 1–2 × 10^6 cells were stimulated with *Staphylococcus* enterotoxin B as a positive control (Sigma, St. Louis, MO), EBV-infected cell extract (Virusys Corporation, Taneytown, MD), or varicella zoster grade 2 antigen (Microbix Biosystems Inc., Ontario, CA) for 2 hr before the addition of Brefeldin A (10 μg/mL, Sigma). After 16 hr of stimulation, cells were washed twice with PBS and stained for flow cytometric analysis.

EBV Viral Titers

Cells were diluted in 1 × RPMI Medium 1640 (Invitrogen) to obtain a final concentration of 1 × 10^6 cells/ml. DNA was extracted with the NucliSens easyMAG system (bioMerieux, Marcy l'Etoile, France) according to the manufacturer's recommendations and eluted with 50 μl elution buffer. EBV quantitative real-time PCR (qPCR) was performed with the Rotor-Gene 3000 instrument (QIAGEN) with amplification and detection of a 192 bp segment from the BamHI-W gene with primers and dual hybridization probes described previously (Feng et al., 2004). The 20 μl reactions consisted of 1 × QuantiTect Probe PCR master mix (QIAGEN) containing HotStarTaq DNA polymerase, reaction buffer, 4.0 mM $MgCl_2$, dNTP mix (containing a dTTP/dUTP mixture), and ROX passive reference dye, and 0.5 μM of each primer, 0.2 μM of each probe, 0.5 U UNG, and 5 μl of extracted DNA. The reaction mixture was preincubated for 10 min at 30°C to activate UNG and then DNA was denatured and UNG inactivated at 95°C for 10 min. The EBV template was first amplified by five cycles of 15 s at 95°C and 40 s at 72°C followed by a touch-down procedure consisting of six cycles of 15 s at 95°C, 30 s at 72°C to 55°C with a 3°C decrease in annealing temperature at each cycle, and 30 s at 72°C. This was then followed by an additional 40 cycles of 15 s at 95°C, 30 s at 55°C, and 30 s at 72°C. Prior to extraction, each sample was spiked with an internal control (pBR322 plasmid DNA) to verify successful recovery of DNA and removal of PCR inhibitors. The internal control in extracted samples was detected by amplification in a separate qualitative real-time PCR as described previously (Cohen et al., 2010). A plasmid containing the EBV amplification sites in pCR2.1 vector (Invitrogen) were linearized and then diluted in TRIS-EDTA buffer (pH 8.0) with glycogen (33.3 μg/ml) to obtain a dilution series for the generation of a standard curve of 5–1 × 10^6 genome copies per reaction volume. For each positive sample, the Rotor-Gene 3000 software plotted the crossing threshold value on this curve to determine the number of target copies present in the amplification reaction.

Statistics

All error bars depict median values. Statistical significance was calculated from the median value with a one- or two-tailed Mann-Whitney test with GraphPad Prism 5.0 software (GraphPad Software Inc., La Jolla, CA). Incidence rates for first occurrence of herpes zoster were determined by dividing the number of cases that occurred during the indicated decade of life by the number of person-years at risk lived during this decade. Exact confidence intervals for these rates were computed based on the assumption that the cases followed a Poisson distribution. Incidence rates for recurrence were calculated by dividing the number of cases of recurrence by the total person years after the first case of herpes zoster among those who already had herpes zoster until the current age or age at recurrence when present. The Kaplan-Meier plot of herpes zoster incidence and statistical significance was calculated with GraphPad Prism 5.0 software.

SUPPLEMENTAL INFORMATION

Supplemental Information includes six figures and can be found with this article online at doi:10.1016/j.immuni.2011.09.016.

ACKNOWLEDGMENTS

The authors would like to thank all of the members of the J.D.M. laboratory for their helpful discussions. We would like to thank the Flow Cytometry Core for all of their sorting assistance. We thank all of the patients and clinical staff whose dedication to human research was invaluable. This work was supported by the intramural research program of the NIAID. A.M.S., J.H., A.P.H., J.M.B., G.H.F., and J.D.M. performed experiments and analyzed data. J.H., A.F.F., S.M.H., and J.D.M. evaluated patients and obtained samples. E.B. performed statistical analysis. J.I.C. and D.C.D. provided sample material and analysis. A.M.S., J.H., and J.D.M. conceived the study, designed experiments, and interpreted data. A.M.S. and J.D.M. wrote the manuscript.

Received: April 15, 2011
Revised: July 26, 2011
Accepted: September 16, 2011
Published online: November 23, 2011

REFERENCES

Akaishi, H., Takeda, K., Kaisho, T., Shineha, R., Satomi, S., Takeda, J., and Akira, S. (1998). Defective IL-2-mediated IL-2 receptor alpha chain expression in Stat3-deficient T lymphocytes. Int. Immunol. *10*, 1747–1751.

Avery, D.T., Deenick, E.K., Ma, C.S., Suryani, S., Simpson, N., Chew, G.Y., Chan, T.D., Palendira, U., Bustamante, J., Boisson-Dupuis, S., et al. (2010). B cell-intrinsic signaling through IL-21 receptor and STAT3 is required for establishing long-lived antibody responses in humans. J. Exp. Med. *207*, 155–171.

Bromberg, J.F., Wrzeszczynska, M.H., Devgan, G., Zhao, Y., Pestell, R.G., Albanese, C., and Darnell, J.E., Jr. (1999). Stat3 as an oncogene. Cell *98*, 295–303.

Buckley, R.H., Schiff, S.E., and Hayward, A.R. (1991). Reduced frequency of CD45RO+ T lymphocytes in blood of hyper-IgE syndrome patients. J. Allergy Clin. Immunol. *87*, 313.

Burke, B.L., Steele, R.W., Beard, O.W., Wood, J.S., Cain, T.D., and Marmer, D.J. (1982). Immune responses to varicella-zoster in the aged. Arch. Intern. Med. *142*, 291–293.

Carrio, R., Bathe, O.F., and Malek, T.R. (2004). Initial antigen encounter programs CD8+ T cells competent to develop into memory cells that are activated in an antigen-free, IL-7- and IL-15-rich environment. J. Immunol. *172*, 7315–7323.

Cohen, J.I., Fahle, G., Kemp, M.A., Apakupakul, K., and Margolis, T.P. (2010). Human herpesvirus 6-A, 6-B, and 7 in vitreous fluid samples. J. Med. Virol. *82*, 996–999.

Conti, H.R., Shen, F., Nayyar, N., Stocum, E., Sun, J.N., Lindemann, M.J., Ho, A.W., Hai, J.H., Yu, J.J., Jung, J.W., et al. (2009). Th17 cells and IL-17 receptor signaling are essential for mucosal host defense against oral candidiasis. J. Exp. Med. *206*, 299–311.

Cui, W., and Kaech, S.M. (2010). Generation of effector CD8+ T cells and their conversion to memory T cells. Immunol. Rev. *236*, 151–166.

Cui, W., Liu, Y., Weinstein, J.S., Craft, J., and Kaech, S.M. (2011). An interleukin-21-interleukin-10-STAT3 pathway is critical for functional maturation of memory CD8$^+$ T cells. Immunity *35*, this issue, 792–805.

de Beaucoudrey, L., Puel, A., Filipe-Santos, O., Cobat, A., Ghandil, P., Chrabieh, M., Feinberg, J., von Bernuth, H., Samarina, A., Jannière, L., et al. (2008). Mutations in STAT3 and IL12RB1 impair the development of human IL-17-producing T cells. J. Exp. Med. *205*, 1543–1550.

Donabedian, H., and Gallin, J.I. (1983). The hyperimmunoglobulin E recurrent-infection (Job's) syndrome. A review of the NIH experience and the literature. Medicine (Baltimore) *62*, 195–208.

Donahue, J.G., Choo, P.W., Manson, J.E., and Platt, R. (1995). The incidence of herpes zoster. Arch. Intern. Med. *155*, 1605–1609.

Douek, D.C., Vescio, R.A., Betts, M.R., Brenchley, J.M., Hill, B.J., Zhang, L., Berenson, J.R., Collins, R.H., and Koup, R.A. (2000). Assessment of thymic output in adults after haematopoietic stem-cell transplantation and prediction of T-cell reconstitution. Lancet *355*, 1875–1881.

Durant, L., Watford, W.T., Ramos, H.L., Laurence, A., Vahedi, G., Wei, L., Takahashi, H., Sun, H.W., Kanno, Y., Powrie, F., and O'Shea, J.J. (2010). Diverse targets of the transcription factor STAT3 contribute to T cell pathogenicity and homeostasis. Immunity *32*, 605–615.

Eddahri, F., Denanglaire, S., Bureau, F., Spolski, R., Leonard, W.J., Leo, O., and Andris, F. (2009). Interleukin-6/STAT3 signaling regulates the ability of naive T cells to acquire B-cell help capacities. Blood *113*, 2426–2433.

Elsaesser, H., Sauer, K., and Brooks, D.G. (2009). IL-21 is required to control chronic viral infection. Science *324*, 1569–1572.

Faulkner, G.C., Burrows, S.R., Khanna, R., Moss, D.J., Bird, A.G., and Crawford, D.H. (1999). X-Linked agammaglobulinemia patients are not infected with Epstein-Barr virus: implications for the biology of the virus. J. Virol. *73*, 1555–1564.

Feng, W.H., Cohen, J.I., Fischer, S., Li, L., Sneller, M., Goldbach-Mansky, R., Raab-Traub, N., Delecluse, H.J., and Kenney, S.C. (2004). Reactivation of latent Epstein-Barr virus by methotrexate: a potential contributor to methotrexate-associated lymphomas. J. Natl. Cancer Inst. *96*, 1691–1702.

Ferwerda, B., Ferwerda, G., Plantinga, T.S., Willment, J.A., van Spriel, A.B., Venselaar, H., Elbers, C.C., Johnson, M.D., Cambi, A., Huysamen, C., et al. (2009). Human dectin-1 deficiency and mucocutaneous fungal infections. N. Engl. J. Med. *361*, 1760–1767.

Foulds, K.E., Rotte, M.J., and Seder, R.A. (2006). IL-10 is required for optimal CD8 T cell memory following *Listeria monocytogenes* infection. J. Immunol. *177*, 2565–2574.

Freeman, A.F., and Holland, S.M. (2010). Clinical manifestations of hyper IgE syndromes. Dis. Markers *29*, 123–130.

Fröhlich, A., Kisielow, J., Schmitz, I., Freigang, S., Shamshiev, A.T., Weber, J., Marsland, B.J., Oxenius, A., and Kopf, M. (2009). IL-21R on T cells is critical for sustained functionality and control of chronic viral infection. Science *324*, 1576–1580.

Glocker, E.O., Hennigs, A., Nabavi, M., Schäffer, A.A., Woellner, C., Salzer, U., Pfeifer, D., Veelken, H., Warnatz, K., Tahami, F., et al. (2009). A homozygous CARD9 mutation in a family with susceptibility to fungal infections. N. Engl. J. Med. *361*, 1727–1735.

Grimbacher, B., Schäffer, A.A., Holland, S.M., Davis, J., Gallin, J.I., Malech, H.L., Atkinson, T.P., Belohradsky, B.H., Buckley, R.H., Cossu, F., et al. (1999). Genetic linkage of hyper-IgE syndrome to chromosome 4. Am. J. Hum. Genet. *65*, 735–744.

Heimall, J., Davis, J., Shaw, P.A., Hsu, A.P., Gu, W., Welch, P., Holland, S.M., and Freeman, A.F. (2011). Paucity of genotype-phenotype correlations in STAT3 mutation positive Hyper IgE Syndrome (HIES). Clin. Immunol. *139*, 75–84.

Holland, S.M., DeLeo, F.R., Elloumi, H.Z., Hsu, A.P., Uzel, G., Brodsky, N., Freeman, A.F., Demidowich, A., Davis, J., Turner, M.L., et al. (2007). STAT3 mutations in the hyper-IgE syndrome. N. Engl. J. Med. *357*, 1608–1619.

Hope-Simpson, R.E. (1975). Postherpetic neuralgia. J. R. Coll. Gen. Pract. *25*, 571–575.

Ichii, H., Sakamoto, A., Hatano, M., Okada, S., Toyama, H., Taki, S., Arima, M., Kuroda, Y., and Tokuhisa, T. (2002). Role for Bcl-6 in the generation and maintenance of memory CD8+ T cells. Nat. Immunol. *3*, 558–563.

Ichii, H., Sakamoto, A., Kuroda, Y., and Tokuhisa, T. (2004). Bcl6 acts as an amplifier for the generation and proliferative capacity of central memory CD8+ T cells. J. Immunol. *173*, 883–891.

Kaech, S.M., Tan, J.T., Wherry, E.J., Konieczny, B.T., Surh, C.D., and Ahmed, R. (2003). Selective expression of the interleukin 7 receptor identifies effector CD8 T cells that give rise to long-lived memory cells. Nat. Immunol. *4*, 1191–1198.

Kallies, A., Xin, A., Belz, G.T., and Nutt, S.L. (2009). Blimp-1 transcription factor is required for the differentiation of effector CD8(+) T cells and memory responses. Immunity *31*, 283–295.

Kimmig, S., Przybylski, G.K., Schmidt, C.A., Laurisch, K., Möwes, B., Radbruch, A., and Thiel, A. (2002). Two subsets of naive T helper cells with distinct T cell receptor excision circle content in human adult peripheral blood. J. Exp. Med. *195*, 789–794.

Klebanoff, C.A., Gattinoni, L., Torabi-Parizi, P., Kerstann, K., Cardones, A.R., Finkelstein, S.E., Palmer, D.C., Antony, P.A., Hwang, S.T., Rosenberg, S.A., et al. (2005). Central memory self/tumor-reactive CD8+ T cells confer superior antitumor immunity compared with effector memory T cells. Proc. Natl. Acad. Sci. USA *102*, 9571–9576.

Kost, R.G., and Straus, S.E. (1996). Postherpetic neuralgia—pathogenesis, treatment, and prevention. N. Engl. J. Med. *335*, 32–42.

Ku, C.C., Murakami, M., Sakamoto, A., Kappler, J., and Marrack, P. (2000). Control of homeostasis of CD8+ memory T cells by opposing cytokines. Science *288*, 675–678.

Kumánovics, A., Perkins, S.L., Gilbert, H., Cessna, M.H., Augustine, N.H., and Hill, H.R. (2010). Diffuse large B cell lymphoma in hyper-IgE syndrome due to STAT3 mutation. J. Clin. Immunol. *30*, 886–893.

Levy, D.E., and Lee, C.K. (2002). What does Stat3 do? J. Clin. Invest. *109*, 1143–1148.

Liu, H., and Rohowsky-Kochan, C. (2011). Interleukin-27-mediated suppression of human Th17 cells is associated with activation of STAT1 and suppressor of cytokine signaling protein 1. J. Interferon Cytokine Res. *31*, 459–469.

Ma, C.S., Chew, G.Y., Simpson, N., Priyadarshi, A., Wong, M., Grimbacher, B., Fulcher, D.A., Tangye, S.G., and Cook, M.C. (2008). Deficiency of Th17 cells in hyper IgE syndrome due to mutations in STAT3. J. Exp. Med. *205*, 1551–1557.

Manjunath, N., Shankar, P., Wan, J., Weninger, W., Crowley, M.A., Hieshima, K., Springer, T.A., Fan, X., Shen, H., Lieberman, J., and von Andrian, U.H. (2001). Effector differentiation is not prerequisite for generation of memory cytotoxic T lymphocytes. J. Clin. Invest. *108*, 871–878.

Migone, T.S., Lin, J.X., Cereseto, A., Mulloy, J.C., O'Shea, J.J., Franchini, G., and Leonard, W.J. (1995). Constitutively activated Jak-STAT pathway in T cells transformed with HTLV-I. Science *269*, 79–81.

Milner, J.D., Brenchley, J.M., Laurence, A., Freeman, A.F., Hill, B.J., Elias, K.M., Kanno, Y., Spalding, C., Elloumi, H.Z., Paulson, M.L., et al. (2008).

Impaired T(H)17 cell differentiation in subjects with autosomal dominant hyper-IgE syndrome. Nature *452*, 773–776.

Minegishi, Y., Saito, M., Tsuchiya, S., Tsuge, I., Takada, H., Hara, T., Kawamura, N., Ariga, T., Pasic, S., Stojkovic, O., et al. (2007). Dominant-negative mutations in the DNA-binding domain of STAT3 cause hyper-IgE syndrome. Nature *448*, 1058–1062.

Nurieva, R.I., Chung, Y., Hwang, D., Yang, X.O., Kang, H.S., Ma, L., Wang, Y.H., Watowich, S.S., Jetten, A.M., Tian, Q., and Dong, C. (2008). Generation of T follicular helper cells is mediated by interleukin-21 but independent of T helper 1, 2, or 17 cell lineages. Immunity *29*, 138–149.

Pellegrini, M., Calzascia, T., Toe, J.G., Preston, S.P., Lin, A.E., Elford, A.R., Shahinian, A., Lang, P.A., Lang, K.S., Morre, M., et al. (2011). IL-7 engages multiple mechanisms to overcome chronic viral infection and limit organ pathology. Cell *144*, 601–613.

Peschon, J.J., Morrissey, P.J., Grabstein, K.H., Ramsdell, F.J., Maraskovsky, E., Gliniak, B.C., Park, L.S., Ziegler, S.F., Williams, D.E., Ware, C.B., et al. (1994). Early lymphocyte expansion is severely impaired in interleukin 7 receptor-deficient mice. J. Exp. Med. *180*, 1955–1960.

Puel, A., Cypowyj, S., Bustamante, J., Wright, J.F., Liu, L., Lim, H.K., Migaud, M., Israel, L., Chrabieh, M., Audry, M., et al. (2011). Chronic mucocutaneous candidiasis in humans with inborn errors of interleukin-17 immunity. Science *332*, 65–68.

Renner, E.D., Rylaarsdam, S., Anover-Sombke, S., Rack, A.L., Reichenbach, J., Carey, J.C., Zhu, Q., Jansson, A.F., Barboza, J., Schimke, L.F., et al. (2008). Novel signal transducer and activator of transcription 3 (STAT3) mutations, reduced T(H)17 cell numbers, and variably defective STAT3 phosphorylation in hyper-IgE syndrome. J. Allergy Clin. Immunol. *122*, 181–187.

Rutishauser, R.L., Martins, G.A., Kalachikov, S., Chandele, A., Parish, I.A., Meffre, E., Jacob, J., Calame, K., and Kaech, S.M. (2009). Transcriptional repressor Blimp-1 promotes CD8(+) T cell terminal differentiation and represses the acquisition of central memory T cell properties. Immunity *31*, 296–308.

Rystedt, I., Strannegard, I.L., and Strannegard, O. (1986). Recurrent viral infections in patients with past or present atopic dermatitis. Br. J. Dermatol. *114*, 575–582.

Sallusto, F., Lanzavecchia, A., Araki, K., and Ahmed, R. (2010). From vaccines to memory and back. Immunity *33*, 451–463.

Scheinberg, P., Melenhorst, J.J., Brenchley, J.M., Hill, B.J., Hensel, N.F., Chattopadhyay, P.K., Roederer, M., Picker, L.J., Price, D.A., Barrett, A.J., and Douek, D.C. (2009). The transfer of adaptive immunity to CMV during hematopoietic stem cell transplantation is dependent on the specificity and phenotype of CMV-specific T cells in the donor. Blood *114*, 5071–5080.

Shin, H., Blackburn, S.D., Intlekofer, A.M., Kao, C., Angelosanto, J.M., Reiner, S.L., and Wherry, E.J. (2009). A role for the transcriptional repressor Blimp-1 in CD8(+) T cell exhaustion during chronic viral infection. Immunity *31*, 309–320.

Speckmann, C., Enders, A., Woellner, C., Thiel, D., Rensing-Ehl, A., Schlesier, M., Rohr, J., Jakob, T., Oswald, E., Kopp, M.V., et al. (2008). Reduced memory B cells in patients with hyper IgE syndrome. Clin. Immunol. *129*, 448–454.

Steininger, C. (2007). Clinical relevance of cytomegalovirus infection in patients with disorders of the immune system. Clin. Microbiol. Infect. *13*, 953–963.

Vogelzang, A., McGuire, H.M., Yu, D., Sprent, J., Mackay, C.R., and King, C. (2008). A fundamental role for interleukin-21 in the generation of T follicular helper cells. Immunity *29*, 127–137.

Winkelstein, J.A., Marino, M.C., Lederman, H.M., Jones, S.M., Sullivan, K., Burks, A.W., Conley, M.E., Cunningham-Rundles, C., and Ochs, H.D. (2006). X-linked agammaglobulinemia: report on a United States registry of 201 patients. Medicine (Baltimore) *85*, 193–202.

Yang, X.O., Panopoulos, A.D., Nurieva, R., Chang, S.H., Wang, D., Watowich, S.S., and Dong, C. (2007). STAT3 regulates cytokine-mediated generation of inflammatory helper T cells. J. Biol. Chem. *282*, 9358–9363.

Yawn, B.P., Saddier, P., Wollan, P.C., St Sauver, J.L., Kurland, M.J., and Sy, L.S. (2007). A population-based study of the incidence and complication rates of herpes zoster before zoster vaccine introduction. Mayo Clin. Proc. *82*, 1341–1349.

Yi, J.S., Du, M., and Zajac, A.J. (2009). A vital role for interleukin-21 in the control of a chronic viral infection. Science *324*, 1572–1576.

Young, T.Y., Jerome, D., and Gupta, S. (2007). Hyperimmunoglobulinemia E syndrome associated with coronary artery aneurysms: deficiency of central memory CD4+ T cells and expansion of effector memory CD4+ T cells. Ann. Allergy Asthma Immunol. *98*, 389–392.

Yu, C.L., Meyer, D.J., Campbell, G.S., Larner, A.C., Carter-Su, C., Schwartz, J., and Jove, R. (1995). Enhanced DNA-binding activity of a Stat3-related protein in cells transformed by the Src oncoprotein. Science *269*, 81–83.